ChemComm

COMMUNICATION

View Article Online
View Journal | View Issue

Cite this: *Chem. Commun.*, 2024, **60**, 5840

Received 18th March 2024,
Accepted 6th May 2024

DOI: 10.1039/d4cc01247j

rsc.li/chemcomm

Mesoporous supraparticles with a tailored solid–liquid–gas interface for visual indication of H_2 gas and NH_3 vapours†

Andreas Zink, ‡[a] Jakob Reichstein, ‡[a] Nico Ruhland,[a] Nina Stockinger,[a] Boris S. Morozov,[b] Carlos Cuadrado Collados,[c] Matthias Thommes,[c] Evgeny A. Kataev,[b] Susanne Wintzheimer[ad] and Karl Mandel *[ad]

Dual-gasochromic supraparticles that undergo rapid eye-readable and gas-specific colour changes upon reaction with hydrogen or ammonia are reported. This functionality is achieved by tailoring the solid–liquid–gas interface within the mesoporous framework of supraparticles *via* spray-drying.

Gasochromic materials that visually indicate the presence of toxic, flammable, or explosive gases through a change in their absorbance become increasingly relevant. Their optical readout facilitates remote and spatially resolved gas detection without a power supply. In addition, optical signal transduction makes an operation in explosive atmospheres possible by eliminating electrical contacts, *i.e.*, the risk of sparks.[1] Hydrogen (H_2) gas and ammonia (NH_3) vapours are currently relevant as targets for gasochromic detectors. They are considered promising energy carriers to foster the decarbonisation of our energy system. However, both gases pose danger to humans due to the high flammability range of H_2/air mixtures[1] and the toxicity of NH_3.[2,3] Therefore, any unintended release during the production, transport, or usage of both gases must be immediately detected and the leakage precisely localized.

A gasochromic particle that can be incorporated as an additive into diverse materials and indicate the presence of both gases through rapid, eye-readable, and gas-specific colour changes at every point of use, *i.e.*, a dual-gasochromic particle, has the potential to meet this demand.

Despite the large variety of gasochromic materials available for H_2 gas[4,5] and NH_3 vapours,[6–8] respectively, no dual-gasochromic particle for these two species has been reported to the best of our knowledge. It is important to mention that electrical dual-gas detectors for H_2 and NH_3[9] or multi-gas detector arrays[7,10] were established but not in the form of one flexibly applicable, gasochromic particle. Most materials for visual H_2 detection are based on the activation of H_2 molecules at catalytically active noble metal surfaces and the subsequent reduction of organic[11] or inorganic chromophores.[4,12] NH_3 vapours are typically detected by impregnating organic pH indicator dyes into porous host materials and exploiting the basic nature of NH_3 as a proton acceptor.[8] Both types of gasochromic materials incorporate functional chromophores into porous support materials. Recently, we introduced supraparticles (SPs) as a new class of (meso)porous support materials for gasochromic indicators.[13] SPs are hierarchical assemblies of nanoparticle (NP) building blocks with a consistent structural motif,[14] offering a highly customizable material design.[13,15–17] The established gasochromic SPs exploit (ir)reversible colour changes of incorporated Reichardt's betaine dye or resazurin (RES) for the detection of NH_3 vapours[13] and H_2 gas,[15–18] respectively. However, the NH_3-indicator SPs cannot detect H_2, and *vice versa*.[18] Thus, the development of a SP for the visual detection of both gases is still an open challenge.

Herein, we report a pioneering example of a dual-gasochromic SP for H_2 gas and NH_3 vapours. Aiming for such a SP, we elaborated a suitable material design that involves the selection of appropriate building blocks and the adjustment of the chemical microenvironment within the solid–liquid–gas interface, provided by the porous framework of the SP. We found that a suitable dye species must undergo distinguishable colour change reactions upon reduction and deprotonation, respectively. Furthermore, we demonstrate that a suitable microenvironment can be created by spray-drying of a mixed dispersion containing SiO_2 NPs, Pt NPs, the chosen dye molecules, and an acid (H_2SO_4),

[a] *Department of Chemistry and Pharmacy, Inorganic Chemistry, Friedrich-Alexander-Universität Erlangen-Nürnberg (FAU), Egerlandstraße 1, D-91058 Erlangen, Germany. E-mail: karl.mandel@fau.de*
[b] *Department of Chemistry and Pharmacy, Organic Chemistry, Friedrich-Alexander-Universität Erlangen-Nürnberg (FAU), Nikolaus-Fiebiger-Str. 10, 91058 Erlangen, Germany*
[c] *Institute of Separation Science and Technology, Friedrich-Alexander-Universität Erlangen-Nürnberg (FAU), Egerlandstraße 3, D-91058 Erlangen, Germany*
[d] *Fraunhofer-Institute for Silicate Research ISC, Neunerplatz 2, D-97082 Würzburg, Germany*

† Electronic supplementary information (ESI) available: Details of experimental section, material characterization. See DOI: https://doi.org/10.1039/d4cc01247j

‡ These authors contributed equally to this work.

functioning as an additional key component. The resulting SPs achieve the targeted functionality through the interaction of H_2 with the incorporated Pt NPs and NH_3 with the acidic liquid phase within the gas-accessible pores of the SP. Both reactions at the solid–gas and liquid–gas interface induce a gas-specific colour change of the comprised dye molecules *via* reduction or deprotonation, respectively. From a broader perspective, the confined space within such mesoporous SPs provides a reaction environment similar to solution chemistry with the following advantages: exotic precursor combinations can be united almost independently of their surface-chemistry using forced assembly. The resulting SP powders can be easily incorporated as active material into sensor devices[19] or as pigment in coatings and clothing.[18]

The first step to create a dual-gasochromic SP for H_2 gas and NH_3 vapours was the identification of suitable chromophore systems and reaction conditions. Therefore, we probed the colour response of various indicator dye solutions by mixing them with NH_3 solution or H_2 gas (Fig. S1, ESI†). The main findings can be summarized as follows: Pt NPs with a size of roughly 5–10 nm (dynamic light scattering, DLS, Fig. S2, ESI†) are required for the H_2-induced reduction of dye molecules by providing active hydrogen at their surface.[11] Many dyes require an acid (*e.g.*, the presence of H_2SO_4) to realize a strong colour change upon reaction with NH_3 solution. An indicator dye species suitable for the envisaged SPs must undergo distinguishable colour responses upon deprotonation, induced by an increase in the pH value of its surrounding medium, and additionally also due to the reduction by active hydrogen. Among all tested indicator dyes (see ESI†), resazurin (RES) and methyl red (MR) are most suitable for the visual indication of both H_2 and NH_3.

In the second step, we created a SP that provides the required chemical microenvironment by forced assembly of the identified key elements, *i.e.*, Pt NPs, dye molecules, H_2SO_4, and framework-building SiO_2 NPs (≈5–15 nm, DLS, Fig. S3, ESI†) *via* spray-drying (Fig. 1A1 and A2). In this process, the different building blocks are united in a mixed dispersion, fed through a nozzle and atomized into small droplets. These droplets enter a hot chamber, which induces the evaporation of the solvent thereby forcing the assembly of all components at the liquid–gas interface, yielding a SP entity. Spray-drying is a continuous, high-throughput and industrially established process, which makes its scalability possible.[20] Herein, we achieved a SP production capacity of 12 g h^{-1} using a lab-scale spray dryer.

For a proof-of-concept study, we exemplary used RES as an indicator dye as it is well studied by others[11] and us.[15–18] We focused in our study on how the addition of H_2SO_4 to the mixed dispersion prior to spray-drying influences the morphology, structure, texture and functionality of the resulting SPs. The mixed dispersion of the reference SP system containing SiO_2 NPs, Pt NPs and RES had a pH ≈ 10 due to the NaOH-stabilisation of the SiO_2 NP dispersion. The other mixed dispersion had a pH ≈ 2 due to the addition of H_2SO_4. The performed spray-drying processes of the two mixed dispersions yielded homogenous, free-flowing powders with a purple and orange colour, respectively (Fig. 1A1 and B1). These colours correspond to the deprotonated (purple) and protonated species of RES (RES-H^+, orange), respectively,[21] matching the colours and UV-vis spectra of the aqueous solutions of RES (Fig. S1, ESI†). Scanning electron microscopy (SEM) imaging (Fig. 1A2 and B2) and laser diffraction measurements (Fig. S4, ESI†) revealed that neither the morphology nor the size

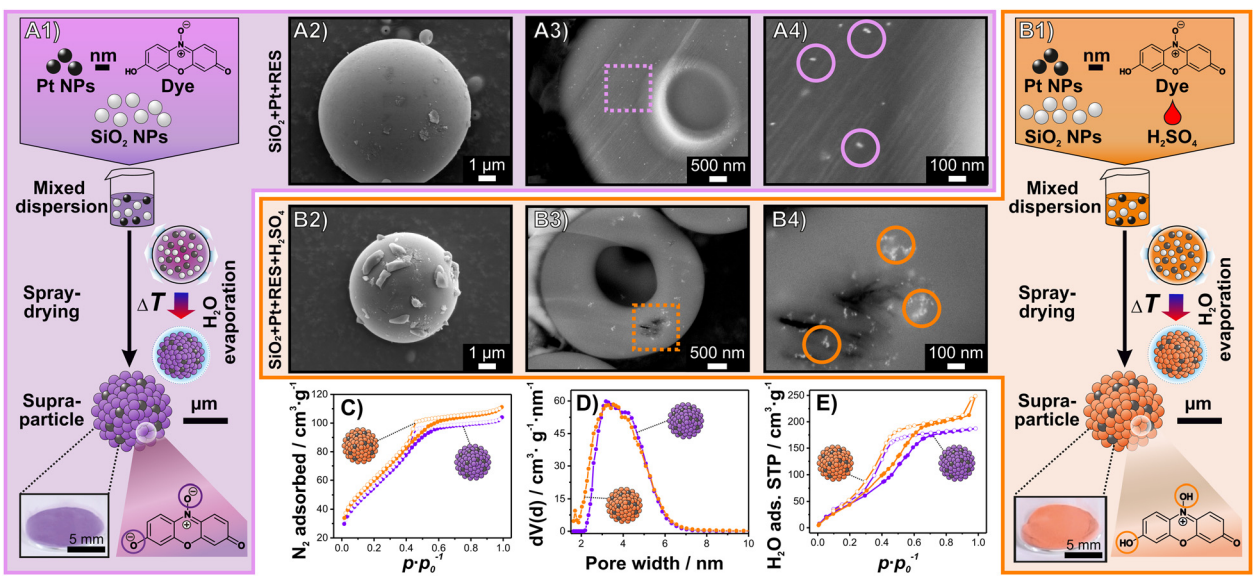

Fig. 1 Synthesis of SPs *via* spray-drying without (A1) and with the addition of H_2SO_4 (B1) and related SEM images of SPs without H_2SO_4 (A2-A4) and with H_2SO_4 (B2-B4): overview images (A2, B2), images of SP cross-sections using backscattered electron detection at different magnifications (A3-4, B3-4). Bright spots partially highlighted with coloured circles indicate the Pt NPs. N_2 ad-/desorption isotherms at 77 K (C). Full symbols indicate adsorption branch and empty symbols indicate desorption branch. Non-local density functional theory (NLDFT) pore size distribution (D). H_2O ad-/desorption isotherms at standard temperature (298 K) and pressure (STP) (E).

distribution of the SPs are significantly altered by the addition of H_2SO_4. Both types of SPs show a spherical or doughnut-like morphology and a size distribution ranging from ≈2 to ≈8 μm. As the Pt NPs are essential for the detection of H_2,[16] we studied their distribution within the SP framework *via* SEM imaging of SP cross-sections using back-scattered electron detecting to obtain elemental contrast. Without the addition of H_2SO_4, the Pt NPs are well dispersed throughout the entire SP (Fig. 1A3) and partially form small agglomerates (Fig. 1A4). In contrast, the addition of H_2SO_4 to the mixed dispersion results in the formation of larger Pt NPs agglomerates within the SP that, in turn, are distributed throughout the entire SP (Fig. 1B3 and B4). The enhanced agglomeration of the citric acid stabilised Pt NPs is attributed to the H_2SO_4-induced destabilisation of the colloidal dispersion.[22]

Similarly, the interstitial pores between the assembled NPs of the SP framework are essential for the targeted functionality.[15] The mesopores are intended to provide the required micro-environment within the solid–liquid–gas interface that consists of solid NPs, liquid pore water that is adsorbed in humid atmospheres[15] and the surrounding gas atmosphere. Therefore, we investigate the effect of the addition of H_2SO_4 to the mixed dispersion prior to spray-drying on the textural properties and the water adsorption capacity of the resulting SPs. Details of the conducted N_2 ad-/desorption at 77 K and H_2O ad-/desorption measurements at 298 K are provided in the ESI† (Fig. S5), while the main findings can be summarized as follows: both SPs are mesoporous, which is indicated by their almost identically shaped type IV N_2 isotherms (Fig. 1C).[23] Their non-local density functional theory (NLDFT) pore size distribution is narrow (≈2–6 nm) with minor differences likely associated with the colloidal destabilization induced by H_2SO_4 (Fig. 1D). Additionally, the presence of H_2SO_4 in the SPs increases the total water adsorption capacity and causes a small shift of the relative pressure range at which water condensation occurs to smaller values (Fig. 1E). We attribute these changes mainly to the hygroscopic nature of H_2SO_4.[24]

Next, we probed the gasochromic functionality of the two SP powder samples by exposing the SP powders to H_2 gas for ≈ 20 s and NH_3 vapours for ≈3 s, respectively – optionally, also after *ex situ* H_2O dosing in a climate chamber (1 h, 30 °C, 98% r.h.) to increase the amount of water in the pores.[15] The SP powder without H_2SO_4 showed the previously reported rapid, eye-readable, two-step (ir)reversible colour change upon H_2 dosing (Fig. 2A1, after *ex situ* H_2O dosing).[15–17] First exposure to H_2 leads to the irreversible reduction of deprotonated RES (purple) to deprotonated resorufin (RF, pink), followed by a reversible reduction to hydroresorufin (hRF, colourless) upon further H_2 dosing (Fig. 2A2). The condensed water in the mesopores grants the mobility of the incorporated dye molecules. This dye mobility enables their migration to the surface of the Pt NPs, where they can be reduced by active hydrogen when H_2 gas is present.[15] SP powder without *ex situ* H_2O dosing did not show a complete conversion to colourless hRF due to a lower dye mobility (Fig. S6, ESI†). However, as the RES molecules in SPs without H_2SO_4 are deprotonated, no colour change is observed upon dosing NH_3 vapours (Fig. 2A3).

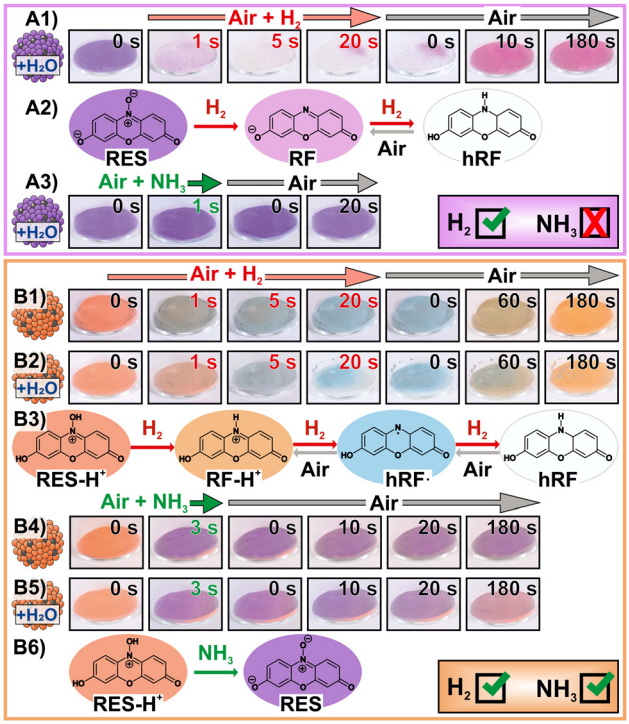

Fig. 2 Gasochromic functionalities of SP powders without (A) and with H_2SO_4 added (B): snapshots before, during and after H_2 dosing of SPs after *ex situ* H_2O dosing (A1) and related reaction network (A2). Snapshots of the same SPs before, during and after NH_3 dosing (A3). Snapshots before, during and after H_2 dosing of SPs containing H_2SO_4 before (B1) and after *ex situ* H_2O dosing (B2) and related reaction network (B3). Snapshots of the same SPs before (B4) and after *ex situ* H_2O dosing (B5) before, during and after NH_3 dosing and related reaction network (B6).

In contrast, SP powder containing Pt NPs, SiO_2 NPs, RES and H_2SO_4 showed rapid, eye-readable, gas-specific colour change reactions upon exposure to H_2 or NH_3 vapours (Fig. 2B, more snapshots provided in Fig. S7, ESI†). First reaction with H_2 irreversibly reduced the orange RES-H^+ to the slightly brighter RF-H^+ (Fig. 2B1–B3). This is confirmed by distinct changes in their absorption and fluorescence spectra (Fig. S8, ESI†). Further H_2 dosing led to blue powder due to the formation of a scarcely reported stable radical state of hRF (hRF, Fig. 2B3).[21] When the dye mobility was high enough, hRF· was further reduced by H_2 dosing to colourless hRF (Fig. 2B2). After stopping H_2 dosing, the colourless SP powder (hRF) turned blue (hRF), before reaching a final orange colour (RF-H^+). It is important to mention that the colouration of these SPs occurred much slower (up to 180 s) compared to their reduction (≈5–10 s) and the colouration of SPs without H_2SO_4 (≈5–10 s). We attribute this slow reversibility to the stability of the blue hRF· radical in air.

In contrast to H_2 dosing, NH_3 vapours induced a rapid, visual colour change of SPs containing H_2SO_4 from orange to purple (Fig. 2B4 and B5) due to deprotonation of RES-H^+ to RES (Fig. 2B6). This reaction is caused by a pH increase of the liquid phase in the mesopores of the SPs that is likely induced by the adsorption and dissolution of gaseous NH_3 species. The

proposed mechanisms are supported by a control SP sample containing SiO_2 NPs, RES, H_2SO_4 but no Pt NPs, which showed no response to H_2 but an identical colour change to NH_3 dosing (Fig. S9, ESI†). The NH_3-induced colour change of the SP powders is partially irreversible, as the initially orange colour related to RES-H^+ was never fully recovered (Fig. 2B4 and B5). Comparing the reversibility of the colour change upon repeated NH_3/air dosing revealed a slightly higher degree of reversibility for SPs after *ex situ* H_2O dosing compared to pristine SPs (Fig. S10, ESI†). The enhanced amount of water after H_2O dosing increases the amount of NH_3 required to alter the pH of the liquid phase in the mesopores.

Besides testing separate H_2 and NH_3 dosing, the SPs containing Pt NPs, SiO_2 NPs, RES and H_2SO_4 were subjected to simultaneous exposure to both target species. Details of this investigation are found in the ESI† (Fig. S11), while the main finding of this investigation can be summarized as follows: NH_3 poisons the incorporated Pt NPs,[25] which results in impaired H_2-induced reduction of the dye species, when both NH_3 and H_2 are present. Therefore, upon dosing of H_2 and NH_3, either pink RF is formed, when H_2 reacts with the SPs first, or deprotonated purple RES, when the SPs react first with NH_3.

Next, we studied the adjustability of the conceptualised SPs and synthesized SPs containing MR as indicator dye. SPs with MR also showed eye-readable, gas-specific colour change reactions upon exposure to H_2 gas or NH_3 vapours (Fig. S12, ESI†). Preliminary quantitative *in situ* UV-vis measurements (Fig. S13, ESI†) demonstrate that dual-gasochromic SPs carrying RES or MR also undergo strong colour changes when they are exposed to $\approx$2 vol% H_2 in N_2 (*i.e.*, below the lower flammability limit of 4 vol%[1]) or $\approx$ 620 ppm NH_3 in N_2 (*i.e.*, below the limit at which human health issues occur[2,3]).

In conclusion, we synthesised and characterised the first dual-gasochromic SPs that undergo rapid, eye-readable, gas-specific colour changes upon reaction with H_2 gas or NH_3 vapours. We revealed the parameters that affect the visual response and characteristics of the SPs. We demonstrated that only SPs assembled from SiO_2 NPs, Pt NPs, suitable dye species (RES or MR) and H_2SO_4, achieve the desired functionality. Thereby, the addition of H_2SO_4 caused just minor changes to the morphology and texture of the SPs but improved the water adsorption capability and ultimately made the desired two gas-specific colour changes *via* scarcely reported reactions possible. The functionality of the SPs results from the synergistic interplay of all four types of building blocks within the solid–liquid–gas interface of their mesoporous framework (Fig. S14, ESI†). This interplay includes the adsorption and condensation of water in the mesopores, the dissociation of H_2 at the surface of Pt NPs and the mobility of incorporated indicator dye molecules in the liquid phase. The later move through and react with the surface of the solid framework, *e.g.*, *via* hydrogenation. Furthermore, we herein demonstrated the possibility of adjusting the pH of the liquid phase in the mesopores during SP synthesis *via* H_2SO_4 addition as well as afterward through the interaction with NH_3 vapours. The dual-gasochromic SPs are therefore a pioneering example for the emergence of new functionalities by exploiting the customisation of the solid–liquid–gas interface within the mesopores of a micron-sized SP.

The contribution of all authors according to the CRediT system is listed in the ESI.† All authors have approved the final version of the manuscript.

This work was financially supported by the BMBF (NanoMatFutur grant 03XP0149 and project IDcycLIB 03XP0393C). J. R. acknowledges his scholarship funding from the German Federal Environmental Foundation (DBU). The authors thank BÜCHI Labortechnik AG for providing the spray dryer equipment.

Conflicts of interest

There are no conflicts to declare.

Notes and references

1 T. Hübert, *et al.*, *Sens. Actuators, B*, 2011, **157**, 329.
2 J. Pauluhn, *Regul. Toxicol. Pharmacol.*, 2013, **66**, 315.
3 L. Silverman, *et al.*, *J. Ind. Hyg. Toxicol.*, 1949, **31**, 74.
4 Y.-A. Lee, *et al.*, *Sens. Actuators, B*, 2017, **238**, 111.
5 (*a*) H. G. Girma, *et al.*, *ACS Sens.*, 2023, **8**, 3004; (*b*) X. Sun, *et al.*, *Appl. Surf. Sci.*, 2022, **599**, 153878.
6 S. Sutthasupa, *et al.*, *Food Chem.*, 2021, **362**, 130151.
7 L. Engel, *et al.*, *Sens. Actuators, B*, 2021, **330**, 129281.
8 A. T. Hoang, *et al.*, *Sens. Actuators, B*, 2016, **230**, 250.
9 (*a*) L. Du, *et al.*, *Sens. Actuators, B*, 2023, **375**, 132873; (*b*) D. D. Roy, *et al.*, *Int. J. Hydrogen Energy*, 2023, **48**, 4931.
10 (*a*) S. H. Lim, *et al.*, *Nat. Chem.*, 2009, **1**, 562; (*b*) J. Chen, *et al.*, *ACS Nano*, 2018, **12**, 6079; (*c*) J. Zhang, *et al.*, *Sens. Actuators, B*, 2021, **326**, 128822; (*d*) Y. Zhang and L.-T. Lim, *Sens. Actuators, B*, 2018, **255**, 3216.
11 M. E. Smith, *et al.*, *Anal. Chem.*, 2020, **92**, 10651.
12 S. Hwan Cho, *et al.*, *Chem. Eng. J.*, 2022, **446**, 136862.
13 S. Wintzheimer, *et al.*, *Part. Part. Syst. Charact.*, 2019, **36**, 1900254.
14 (*a*) S. Wintzheimer, *et al.*, *ACS Nano*, 2018, **12**, 5093; (*b*) J. Reichstein, *et al.*, *Adv. Mater.*, 2023, **35**, e2306728.
15 J. Reichstein, *et al.*, *Adv. Funct. Mater.*, 2022, **32**, 2112379.
16 K. Zhang, *et al.*, *Chem. Mater.*, 2023, **35**, 6808.
17 K. Zhang, *et al.*, *J. Chem. Phys.*, 2023, **158**, 134722.
18 J. Reichstein, *et al.*, *Adv. Mater. Technol.*, 2024, 2400441.
19 C. Pannek, *et al.*, *Sens. Actuators, B*, 2020, **306**, 127572.
20 (*a*) D. P. Debecker, *et al.*, *Chem. Soc. Rev.*, 2018, **47**, 4112; (*b*) S. Wintzheimer, *et al.*, *Adv. Mater.*, 2023, **35**, e2306648.
21 S. Khazalpour and D. Nematollahi, *RSC Adv.*, 2014, **4**, 8431.
22 G. Marzun, *et al.*, *Langmuir*, 2014, **30**, 11928.
23 M. Thommes, *et al.*, *Pure Appl. Chem.*, 2015, **87**, 1051.
24 K. B. Kiradjiev, *et al.*, *Ind. Eng. Chem. Res.*, 2020, **59**, 4802.
25 D. A. Finkelstein, *et al.*, *J. Phys. Chem. C*, 2015, **119**, 9860.